ELSEVIER

Neurobiology of Aging 33 (2012) 2018–2028

NEUROBIOLOGY OF AGING

www.elsevier.com/locate/neuaging

Resting-state fMRI changes in Alzheimer's disease and mild cognitive impairment

Maja A.A. Binnewijzend[a,*], Menno M. Schoonheim[a,b], Ernesto Sanz-Arigita[a,1], Alle Meije Wink[a], Wiesje M. van der Flier[c], Nelleke Tolboom[d], Sofie M. Adriaanse[d], Jessica S. Damoiseaux[e], Philip Scheltens[c], Bart N.M. van Berckel[d], Frederik Barkhof[a]

[a] Department of Radiology, VU University Medical Center, Amsterdam, The Netherlands
[b] Department of Anatomy and Neuroscience, VU University Medical Center, Amsterdam, The Netherlands
[c] Department of Neurology, VU University Medical Center, Amsterdam, The Netherlands
[d] Department of Nuclear Medicine and PET Research, VU University Medical Center, Amsterdam, The Netherlands
[e] Department of Neurology and Neurological Sciences, Stanford University School of Medicine, Palo Alto, CA, USA

Received 27 March 2011; received in revised form 14 June 2011; accepted 7 July 2011

Abstract

Regional functional connectivity (FC) of 39 patients with Alzheimer's disease (AD), 23 patients with mild cognitive impairment (MCI), and 43 healthy elderly controls was studied using resting-state functional magnetic resonance imaging (rs-fMRI). After a mean follow-up of 2.8 ± 1.9 years, 7 MCI patients converted to AD, while 14 patients remained cognitively stable. Resting-state functional magnetic resonance imaging scans were analyzed using independent component analysis (ICA), followed by a "dual-regression" technique to create and compare subject-specific maps of each independent spatiotemporal component, correcting for age, sex, and gray matter atrophy. AD patients displayed lower FC within the default-mode network (DMN) in the precuneus and posterior cingulate cortex compared with controls, independent of cortical atrophy. Regional FC values of MCI patients were numerically in between AD patients and controls, but only the difference between AD and stable MCI patients was statistically significant. Correlation with cognitive dysfunction demonstrated the clinical relevance of FC changes within the DMN. In conclusion, clinically relevant decreased FC within the DMN was observed in AD.

Keywords: Functional connectivity; Default mode network; Clinical follow-up; Cognition

1. Introduction

Alzheimer's disease (AD) is a progressive neurodegenerative disorder. The hallmark of AD on magnetic resonance imaging (MRI) is atrophy, mainly located in the medial temporal and parietal cortices (Sluimer et al., 2009). With the prospect of disease-modifying therapies it is desirable to detect signs of neurodegeneration at an early stage of the disease, before neuronal cell destruction is detectable on MRI as atrophy.

Molecular markers, e.g., amyloid binding positron emission tomography (PET) tracer uptake and abnormally reduced cerebrospinal fluid (CSF) amyloid-β_{42}, show the earliest detectable changes in the course of AD. However, amyloid plaque deposition occurs prior to cognitive decline and reaches a plateau in a very early stage of the clinical disease (Frisoni et al., 2010; Jack et al., 2009). In the absence of structural damage reflected by volume loss on MRI, functional markers, such as glucose metabolism representing ^{18}F-fluorodeoxyglucose (FDG) PET, are more suitable to monitor disease progression because functional

* Corresponding author at: Department of Radiology, VU University Medical Center, PO Box 7057, 1007 MB Amsterdam, The Netherlands. Tel.: +31 20 444 0685; fax: +31 20 444 0397.
E-mail address: m.binnewijzend@vumc.nl (M.A.A. Binnewijzend).
[1] Present address: Department of Radiology, Foundation CITA-AD, Parque Tecnológico de San Sebastián, P° Mikeletegi 61, 20009 Donostia-San Sebastián, Spain.

0197-4580/$ – see front matter © 2012 Elsevier Inc. All rights reserved.
10.1016/j.neurobiolaging.2011.07.003

changes are present in an early stage of the disease and continue to change as the disease progresses.

Resting-state functional MRI (rs-fMRI) is an imaging method that reflects synaptic activity through changes in blood flow and the oxyhemoglobin:deoxyhemoglobin ratio (Schölvinck et al., 2010). In contrast to ^{18}F-fluorodeoxyglucose-PET, it is a noninvasive technique that is widely available. By measuring functional connectivity (FC) between spatially distinct brain regions rs-fMRI can be used to evaluate brain function (Biswal et al., 1995; Cordes et al., 2001). Several networks encompassing brain regions that display FC during resting state, so-called resting state networks (RSNs), have been described previously (Beckmann et al., 2005; Damoiseaux et al., 2006, 2008). One network is referred to as the "default mode network" (DMN) and consists of the bilateral parietal cortex, the precuneus and posterior cingulate cortex (PCC), anterior cingulate cortex (ACC), medial prefrontal cortex (MPFC), hippocampus, and thalamus. The network is active during episodical and autobiographical memory retrieval but shows a decreased activity during the performance of cognitive tasks that demand attention to external stimuli (Greicius et al., 2003, 2004; Raichle et al., 2001). Interestingly, structures that are particularly vulnerable for early amyloid deposition in AD appear to overlap with the heteromodal cortices of the DMN (Buckner et al., 2009).

Previous rs-fMRI studies have shown a disruption in FC between structures that are part of the DMN at an early stage of AD and mild cognitive impairment (MCI) (Greicius et al., 2004; He et al., 2007; Sorg et al., 2007; Wang et al., 2006, 2007; Zhang et al., 2009). Many studies used a seed-based approach to analyze functional MRI data. This method requires an a priori definition of regions of interest ("seed regions") making it very suitable for specific hypotheses about a particular brain structure. However, exploring FC differences within a specific RSN requires different analysis methods.

In this study we used the "dual-regression" analysis technique (Filippini et al., 2009) that has previously been applied successfully in different neurological conditions other than AD (Cole et al., 2010; Roosendaal et al., 2010). Unlike other back-reconstruction techniques, the dual-regression technique takes both spatial and temporal information of the RSN into account to create subject-specific temporo-spatial maps. We used these subject-specific spatial maps to investigate the differences in FC within the RSNs, mainly focusing on the DMN, in a voxel-wise fashion between AD patients, MCI patients, and healthy elderly controls. Secondly, we investigated if conversion to AD at follow-up was related to lower FC in MCI patients at baseline. Finally, we studied whether FC values within these regions of lower FC correlated with cognitive decline in AD.

2. Methods

2.1. Subjects

One hundred five subjects were included in this study: 39 patients with AD, 23 patients with MCI, and 43 controls. The data set was formed by combining 2 data sets of functional MRI (fMRI) data that were scanned using the same protocol (Damoiseaux et al., 2008; Tolboom et al., 2009). Patients were recruited from the Alzheimer Center of the VU University Medical Center, Amsterdam, The Netherlands. All patients received a standard dementia screening that included medical history, physical and neurological examinations, and screening laboratory tests, and extensive neuropsychological testing and brain MRI. Clinical diagnosis was established by a multidisciplinary team. AD patients met the NINCDS-ADRDA (National Institute of Neurological and Communicative Disorders and Stroke and the Alzheimer's Disease and Related Disorders Association) criteria for "probable AD" (McKhann et al., 1984) and had Mini Mental State Examination (MMSE) scores $\geq$ 17 (range, 17–27). MCI patients met the Petersen criteria based on subjective and objective cognitive impairment, predominantly affecting memory, in the absence of dementia or significant functional loss (Petersen et al., 2001), and had a clinical dementia rating (CDR) score of 0.5 (Morris, 1993). Controls consisted of family members of patients and volunteers recruited through advertisements posted in the Alzheimer Center and activity centers for the elderly in the community. The Ethical Review Board of the VU University Medical Center Amsterdam approved the study. Written informed consent was provided by all subjects or their lawful caregiver. Exclusion criteria included significant medical, neurological (other than AD), or psychiatric illness; a history of brain damage; and use of non AD-related medication known to influence cerebral function such as benzodiazepines and antidepressants.

2.2. Neuropsychological assessment

A subset of 91 subjects underwent extensive neuropsychological assessment, including MMSE (Folstein et al., 1975), Digit Span (Wechsler, 1997), immediate and delayed recall of the Dutch version of the Rey Auditory Verbal Learning Task (RAVLT) (Rey, 1964), Visual Association Test (VAT; ranging from 1 to 12) together with VAT picture naming (Lindeboom et al., 2002), category fluency, Trail Making Test part A and B, Stroop tests with the Word, Color, and Color-Word subtasks (Stroop, 1935), and the Rey Complex Figure Copy test (Osterrieth, 1944).

2.3. Follow-up

Diagnostic classification of MCI patients was re-evaluated annually at the memory clinic. Mean follow-up time of 21 MCI patients was 2.8 years (2.8 $\pm$ 1.9). During this period, 7 MCI patients converted to AD (cMCI), whereas 14 MCI patients remained cognitively stable (sMCI). One MCI patient

converted to dementia caused by frontotemporal lobar degeneration (FTLD) (Neary et al., 1998), while in another MCI patient no follow-up information could be retrieved. These latter 2 patients were left out of further analyses between cMCI and sMCI patients.

2.4. Data acquisition

Imaging was performed on a 1.5 Tesla Siemens Sonata scanner (Siemens AG, Erlangen, Germany) using a standard circularly polarized head coil (gradient 40 mT/m, slew rate 200 T/m per second). Resting state functional scans consisted of 200 T2*-weighted echo planar imaging (EPI) volumes (repetition time = 2850 ms; echo time = 60 ms; flip angle = 90°; 36 axial slices; matrix 64 × 64; voxel size 3.3 mm isotropic). Subjects were instructed to lie still with their eyes closed, not to think of any 1 thing in particular and not to fall asleep during the resting state scan. Additionally a high-resolution T1-weighted magnetization prepared rapid acquisition gradient echo (MPRAGE) image (repetition time = 2700 ms; echo time = 3.97 ms; inversion time = 950 ms; flip angle = 8°; 160 coronal slices; matrix 256 × 192; voxel size 1 × 1.5 × 1 mm) was acquired.

2.5. Analysis of resting-state data

Data analyses were carried out using MELODIC of FMRIB's Software Library (FSL version 4.1; www.fmrib.ox.ac.uk/fsl) to identify large-scale patterns of temporal signal-intensity coherence, interpreted as FC, in the population of subjects (Beckmann et al., 2005). Preprocessing consisted of motion correction, removal of nonbrain tissue, spatial smoothing using a 5 mm full-width-at-half-maximum Gaussian kernel, and high-pass temporal filtering equivalent to 100 seconds (0.01 Hz). After preprocessing the fMRI volumes were registered to the subject's high-resolution T1-weighted scan using affine registration and subsequently to standard space (MNI152) images using nonlinear registration with a warp resolution of 10 mm. Subsequently the data of all above-mentioned subjects were temporally concatenated across subjects to create a single 4-dimensional data set. The data set was decomposed into independent components, with a free estimation for the number of components. Model order was estimated using the Laplace approximation to the Bayesian evidence for a probabilistic principal component model. Components of interest were selected by visual inspection based on previous literature (Beckmann et al., 2005; Damoiseaux et al., 2006) and the frequency spectra of the time courses of the components.

For between-subject analyses a voxel-wise comparison of the resting FC was carried out using a regression technique referred to as the "dual-regression" approach (Filippini et al., 2009). Spatial maps of the group independent component analysis (ICA) were used in a linear model fit against each individual fMRI data set (spatial regression), to create matrices that described the temporal dynamics for each component and subject separately. These matrices were used in a linear model fit against the associated subject's fMRI data set (temporal regression), to estimate subject-specific spatial correlation maps. After this dual regression, spatial maps of all subjects were collected into single 4-dimensional files for each original independent component. Nonparametric permutation tests (5000 permutations) were used to detect statistically significant differences between the groups within the boundaries of the spatial maps obtained with MELODIC, correcting for age, sex and origin of data set (Nichols and Holmes, 2002). Finally, a family-wise error (FWE) correction for multiple comparisons was performed, implementing threshold-free cluster enhancement (TFCE) using a significance threshold of $p < 0.05$ (Smith and Nichols, 2009). The regions that showed differences in FC between groups were used to extract mean z-values from each individual spatial map (FWE-corrected $p < 0.05$).

Gray matter volume, normalized for subject head size (NGMV), was estimated using SIENAX (Smith et al., 2002), part of FSL 4.1. To correct for the effect of cortical atrophy, a second dual-regression analysis was carried out on the networks that previously showed FC changes, using gray matter volume loss as an additional covariate in the permutation tests.

2.6. Nonimaging statistics

All other statistical analyses were performed using SPSS (version 15.0; SPSS, Chicago, IL, USA). Data of Trail Making Test (TMT) and Stroop tests were log transformed as Kolmogorov-Smirnov tests showed they were not normally distributed. For continuous measures, differences between groups were assessed using 1-way analysis of variance (ANOVA) with post hoc Bonferroni tests to correct for multiple comparisons. A χ^2 test was used to compare frequency distributions of sex. Linear regression analyses were performed across the diagnostic groups and within the patient groups to assess relationships between regional FC within the DMN (independent variable; extracted mean z-values from clusters of regional differences) and neuropsychological test results (dependent variables) with adjustment for age and sex, and, additionally, for gray matter atrophy.

3. Results

3.1. Demographics and cognitive performance

No differences in age, sex, or level of education were found between the 3 diagnostic groups (Table 1). As expected, MMSE scores differed between all groups. AD patients showed a decrease in NGMV compared with controls (756 ± 52 vs. 811 ± 46 cc; $p < 0.001$). No differences in NGMV were found between controls and MCI (784 ± 49

Table 1
Demographics and neuropsychological test outcomes

	Control	MCI	AD	*p* value
Demographics				
n (total *n* = 105)	43	23	39	
Age, y	69 ± 7	71 ± 8	67 ± 8	0.229
Sex (% female)	47	35	41	
Education [a]	6 ± 1	6 ± 1	5 ± 1	0.201
MMSE	29 ± 1	27 ± 3*	22 ± 3*,**	<0.001
Neuropsychological test outcomes				
n (total *n* = 91)	38	23	30	
Digit span, forward [b]	13 ± 3	14 ± 2	11 ± 3*,**	0.006
Digit span, backward [b]	10 ± 3	10 ± 3	7 ± 3*,**	0.003
TMT A [b,c]	41 ± 17	43 ± 13	80 ± 35*,**	<0.001
Stroop, word [b,c]	45 ± 6	47 ± 10	57 ± 18*,**	<0.001
Stroop, color [b,c]	60 ± 11	64 ± 18	90 ± 44*,**	<0.001
Stroop, color-word [c,d]	112 ± 34	119 ± 32	170 ± 63*,**	<0.001
RAVLT immediate recall	42 ± 11	26 ± 7*	21 ± 7*	<0.001
RAVLT delayed recall	8 ± 3	2 ± 2*	1 ± 2*	<0.001
VAT [b]	12 ± 1	10 ± 3*	4 ± 4*,**	<0.001
VAT picture naming [d]	12 ± 1	12 ± 1	11 ± 2*	0.019
TMT B [c,d]	91 ± 39	113 ± 29	240 ± 179*,**	<0.001
Category fluency [b]	23 ± 5	19 ± 6*	12 ± 4*,**	<0.001
Rey figure copy [d]	34 ± 3	33 ± 5	25 ± 9*,**	<0.001

Data are presented as means ± standard deviations. If analysis of variance was $p < 0.05$ a post hoc Bonferroni test was performed.
Key: AD, Alzheimer's disease; MCI, mild cognitive impairment; MMSE, Mini Mental State Examination; RAVLT, Rey Auditory Verbal Learning Task; TMT, Trail Making Test; VAT, Visual Association Task.
[a] Level of education using Verhage's classification (Verhage, F., 1964).
[b] Missing data of 1–3 subjects.
[c] Lower scores indicate better (faster) performance.
[d] Missing data of 4–8 subjects.
* $p < 0.05$ compared with controls.
** $p < 0.05$ compared with MCI patients.

cc; $p = 0.12$), or between MCI and AD ($p = 0.09$). Cognitive performance of controls and AD patients differed on all neuropsychological tests, with AD patients showing poorest test results (Table 1). Performance of MCI patients and AD patients differed on all tests except for the RAVLT (immediate and delayed recall) and VAT picture naming, with MCI patients showing better test results than AD patients. Controls and MCI patients only differed on the RAVLT (immediate and delayed recall), VAT, and category fluency test.

3.2. Resting state network identification

The group ICA estimated 27 components. Based on their frequency spectra, their spatial patterns and on previous literature (Beckmann et al., 2005; Damoiseaux et al., 2006, 2008) 10 components were found to represent functional RSNs. Peak of the frequency spectra of all of these components was below 0.03 Hz. The remaining 17 components reflected artifacts like movement, physiological noise, and cerebrospinal fluid flow. Fig. 1 shows an overview of the functional RSNs, consisting of right and left working memory network (a and e), dorsal visual-spatial attention system (b), primary and secondary visual areas (g and c), basal ganglia and cerebellum (d), sensory and motor function (f), auditory and language processing (h), the default mode network (i), and ventral spatial attention system (j). In our sample the default mode network (Fig. 1i) consisted of bilateral lateral parietal cortex, precuneus and PCC, ACC, medial prefrontal cortex, bilateral operculum, medial temporal cortex, lateral temporal cortex, and the thalamus.

3.3. Functional connectivity changes

Within the DMN, 4 regions of lower FC were found in AD compared with controls within the precuneus and the PCC (Fig. 2; FWE-corrected $p < 0.05$) (Table 2). The 2 largest of these regions (precuneus and cuneus) remained significant when repeating the dual regression analysis using NGMV as an additional covariate (FWE-corrected $p < 0.05$). No regions of FC changes were found within the DMN when comparing MCI patients with controls or AD patients. No regions of higher FC in AD patients compared with controls were found.

Two other RSNs showed regions of lower FC in AD (Table 2). The secondary visual network displayed 1 region of lower FC in AD patients compared with controls in the right occipital lobe (Fig. 3a). This cluster did not survive the statistical threshold when correcting for gray matter atrophy. The basal ganglia and cerebellum network (Fig. 3b) showed 5 regions of lower FC in AD patients compared with controls in the right thalamus, the right putamen, and the right and left hemisphere of the cerebellum. Three of these regions survived correction for gray matter atrophy.

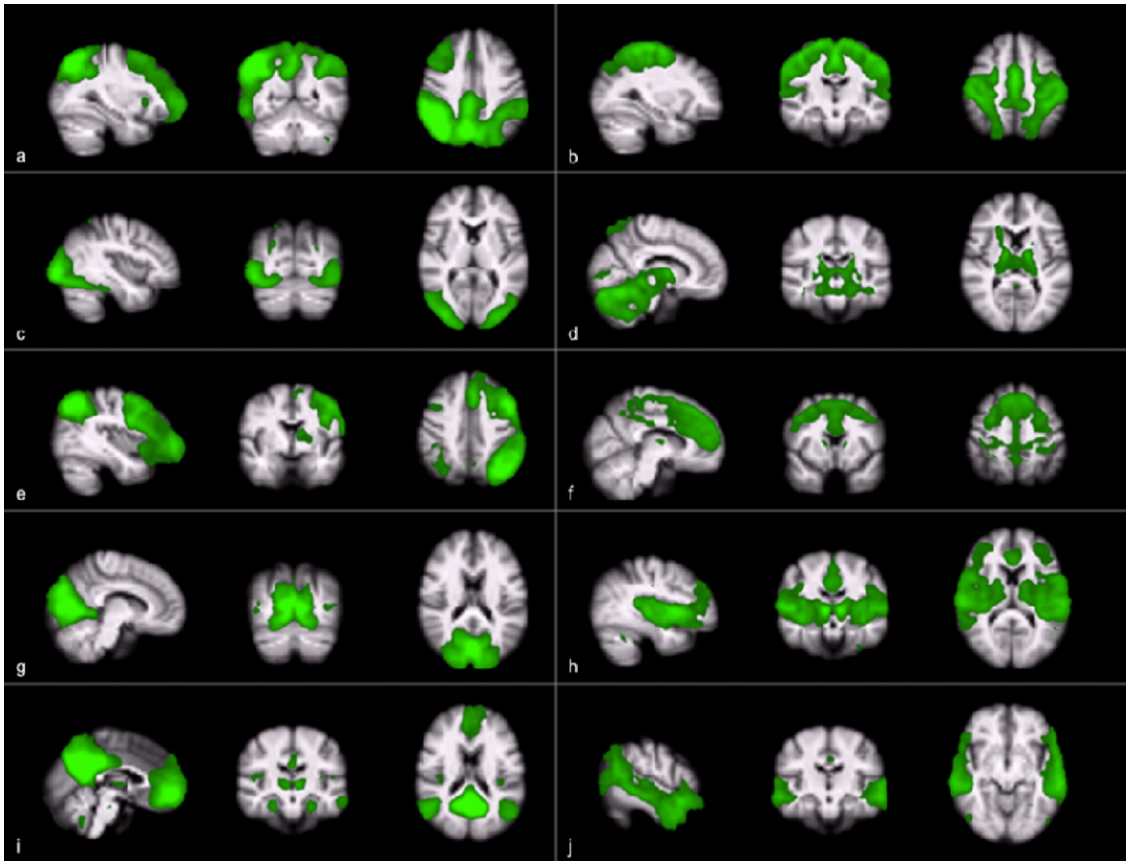

Fig. 1. (a) Right working memory (x = 31, y = −52, z = 39), (b) dorsal visual-spatial attention system (x = 30, y = −16, z = 48), (c) secondary visual areas (x = 38, y = −73, z = 8), (d) basal ganglia and cerebellum (x = 10, y = −17, z = 10), (e) left working memory (x = −39, y = −1, z = 43), (f) sensory and motor function (x = 8, y = 12, z = 52), (g) primary visual areas (x = 7, y = −74, z = 19), (h) auditory and language processing (x = −37, y = −14, z = 12), (i) the default-mode network (including thalamus and hippocampus; x = −1, y = −17, z = 19), and (j) ventral spatial attention system (x = −54, y = −17, z = −7). The images (sagittal, coronal and axial view) are z-statistics overlaid on the average high-resolution scan transformed into standard (MNI152) space. Dark green to light green are *z*-values ranging from 2.3 to 10.0. The left hemisphere of the brain corresponds to the right side of the image.

The regions of lower DMN FC in AD patients compared with controls (cuneus, precuneus, and the PCC; FWE-corrected $p < 0.05$) were used as regions-of-interest to extract the average *z*-values from the subject-specific spatial maps of all subjects (Fig. 2). Fig. 4 shows a box plot of the mean *z*-values of FC in the patient groups in these regions. Mean *z*-values of MCI patients (4.9 ± 1.1) were numerically in between AD patients (4.3 ± 1) and controls (5.5 ± 1.1) but did not reach significance when comparing regional DMN FC values with AD ($p = 0.09$) and controls ($p = 0.17$). After exclusion of 1 outlier from the control group ($z = 2.1$; > 3 SD below the mean), there was a trend toward significance in regional FC between MCI patients and controls ($p = 0.07$).

3.4. Comparing stable and converting MCI patients

No differences in age ($p = 1.00$), sex ($p = 0.77$), level of education ($p = 1.00$), MMSE scores ($p = 1.00$), NGMV ($p = 0.51$), and neuropsychological test scores were found between sMCI and cMCI patients. Regional FC (i.e., within the region of lower FC between AD and controls) did not differ between sMCI and cMCI (5.0 ± 1.1 vs. 4.8 ± 1.0) (Fig. 4). Using independent samples *t* tests, connectivity values of sMCI patients differed from those of AD patients ($p = 0.03$), while no significant differences between sMCI patients and controls were found ($p = 0.21$). Regional FC values of cMCI patients did not reach significance compared with those of controls ($p = 0.14$) or AD patients ($p = 0.27$).

3.5. Correlation with cognition

Across the diagnostic groups, linear regression analyses displayed that lower regional FC within the DMN was associated with lower scores on MMSE (standardized $\beta = 0.41$; $p < 0.001$). Furthermore, associations between lower regional FC and worse test performance were found for Digit Span (backward), Stroop word and Stroop color-word test, TMT (A and B), VAT, RAVLT (immediate and de-

Fig. 2. Green voxels represent the group default mode network (DMN). Blue voxels show clusters of decreased functional connectivity (FC) in Alzheimer's disease (AD) compared with controls ($p < 0.05$ family-wise error [FWE]-corrected). Montreal Neurological Institute (MNI) coordinates x = 4, y = −59, z = 29. (a) Results are corrected for age, sex, and origin of data set. These clusters were used as region-of-interest to extract mean z-values of FC from each individual independent component map. (b) Results are corrected for age, sex, origin of data set, and normalized gray matter volume.

layed), Category Fluency, and Rey Figure Copy test (Table 3). Within AD, we found a strong correlation between DMN FC values and Rey Figure Copy Test outcomes (standardized $\beta = 0.61$; $p = 0.002$). No other correlations were found within the AD patient group. No correlations were found within the control and the MCI group. When applying an additional correction for gray matter atrophy the results remained essentially unchanged.

Table 2
Decreased FC clusters in AD compared with controls

Voxels, *n*	*p*-value	MNI coordinates			Location
		x	y	z	
Default mode network					
31	0.01	−2	−62	4	Precuneus, cuneus
17	0.01	2	−46	28	Left and right precuneus
3	0.04	−2	−62	32	Left precuneus
3	0.04	2	−34	28	PCC
After gray matter atrophy correction					
2	0.04	14	−58	4	Right cuneus
3	0.02	−2	−62	4	Left cuneus
3	0.04	2	−50	28	Precuneus
Secondary visual network					
4	0.02	30	−94	20	Right occipital cortex
Basal ganglia and cerebellum					
7	0.03	22	−26	12	Right thalamus
5	0.01	30	−14	−4	Right putamen
6	0.02	26	−62	−36	Right hemisphere cerebellum
1	0.05	30	−54	−40	Right hemisphere cerebellum
1	0.05	−22	−74	−32	Left hemisphere cerebellum
After gray matter atrophy correction					
7	0.01	22	−26	8	Right thalamus
3	0.01	30	−14	−4	Right putamen
10	0.02	26	−62	−36	Right hemisphere cerebellum

p values are family-wise error (FWE)-corrected.
Key: MNI, Montreal Neurological Institute; PCC, posterior cingulate.

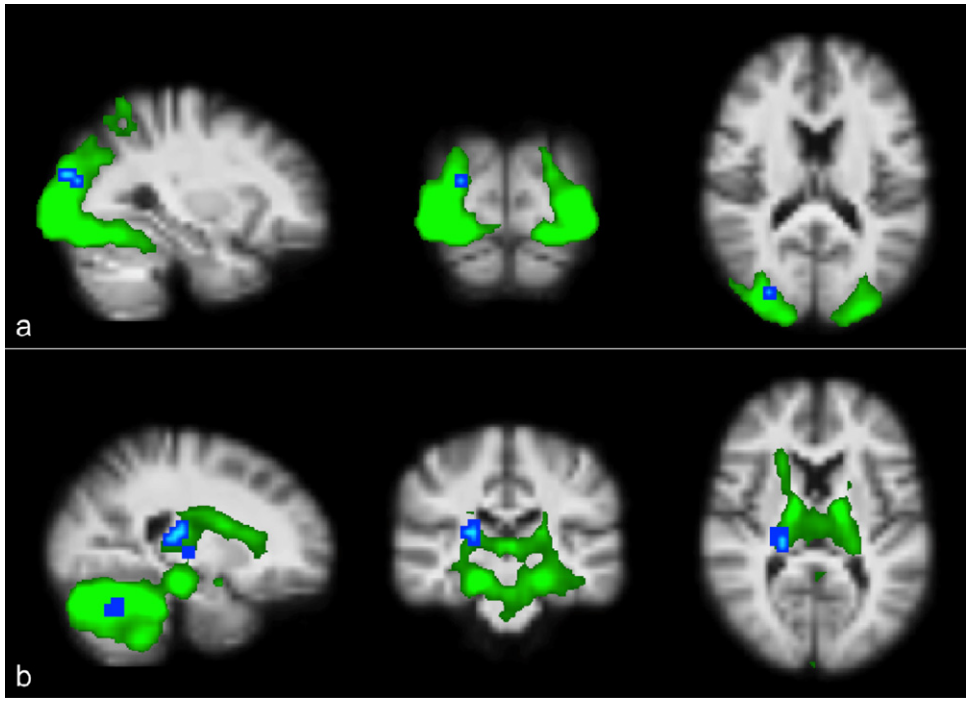

Fig. 3. Green voxels represent the group resting state networks (RSNs), i.e., (a) the secondary visual network (Montreal Neurological Institute [MNI] coordinates x = 30, y = −87, z = 17) and (b) the network of basal ganglia and cerebellum (MNI coordinates x = 22, y = −25, z = 10). Blue voxels show clusters of significantly lower FC in AD compared with controls ($p < 0.05$, family-wise error [FWE]-corrected). Results are corrected for age, sex, and origin of data set.

4. Discussion

In this study we found regions of lower FC in AD patients compared with controls within the DMN, located in the precuneus and posterior cingulate cortex. Regional FC values of MCI patients were numerically in between AD patients and controls. Furthermore, AD patients displayed a lower regional FC than sMCI patients while no differences in regional FC were found between cMCI and AD patients. Reduced FC was correlated with cognitive dysfunction both across diagnostic groups and within the AD group.

To detect regional differences in FC between AD patients, MCI patients, and controls, a group ICA was executed resulting in 27 independent components of which 10 were recognized as RSNs. Subsequently, a newly developed dual-regression analysis technique was applied to compare subject-specific spatial maps of each independent component. This technique uses the group ICA component maps to back-reconstruct the group spatial maps into subject-specific temporospatial maps by applying 2 regression analyses taking both temporal coherence and spatial similarity of the component into account. This provides an advantage over techniques that select and match subject-specific components based on their spatial similarity (e.g., "goodness-of-fit") after having applied single subject ICAs, in which similarity in temporal signal intensity coherence cannot be assured. A possible future advantage of the dual-regression analysis is the possibility to omit doing an ICA to create group-specific RSN masks and use standardized masks of RSNs obtained from very large samples of subjects instead. Once such masks are available, this will provide even more standardized results that will be comparable across different data sets because results do not depend on group-specific independent component masks.

Voxel-wise comparisons of the obtained individual RSN maps displayed FC changes between AD patients and controls in 3 of the networks, including the DMN. All regions of lower DMN FC were located in the posteromedial part of the network, a region that is particularly vulnerable for amyloid pathology at an early stage of the disease.

These regions survived correction for gray matter volume loss, confirming that lower DMN FC in AD reflects functional changes within the cortical tissue. This is in line with the results of other studies applying a correction for the effect of cortical atrophy (Bai et al., 2008; He et al., 2007; Sorg et al., 2007). The fact that the regions of DMN FC differences were smaller after correction for gray matter volume loss illustrates that the lower DMN FC in AD can be partly explained by the loss of cortical brain tissue.

Several other studies that cross-sectionally investigated FC within the DMN or between brain regions that are part of the DMN found similar results (Bai et al., 2008; Greicius et al., 2004; Qi et al., 2010; Sorg et al., 2007; Zhang et al., 2009). Studies using seed-based analyses of the precuneus/PCC demonstrated decreased connectivity between the pre-

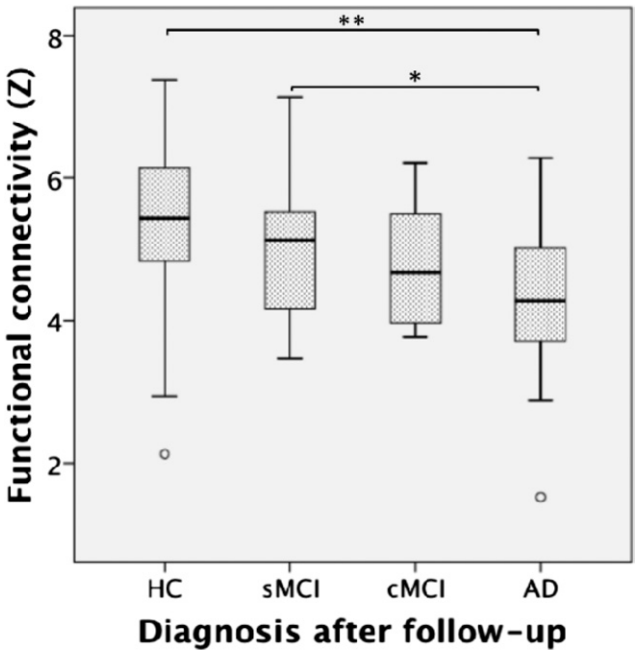

Fig. 4. Mean z-values were extracted for each subject from the individual default-mode network (DMN) z-maps obtained from the dual regression analysis and compared using independent-samples t tests. Abbreviations: AD, Alzheimer's disease; FC, functional connectivity; HC, healthy control. * $p < 0.05$; ** $p < 0.001$.

cuneus/PCC and several brain regions, including (medial) temporal cortex, hippocampus, prefrontal cortex, and thalamus (Bai et al., 2009; Wang et al., 2007; Zhang et al., 2009). Independent component analyses have been used to investigate differences in DMN connectivity in earlier and later stage AD, showing decreased connectivity in precuneus/PCC, as well as in hippocampus, lateral parietal, and medial prefrontal cortices (Greicius et al., 2004; Qi et al., 2010; Sorg et al., 2007; Zhou et al., 2010).

The posteromedial regions, together with the lateral parietal cortices, are particularly vulnerable for early AD pathology, with amyloid pathology being located in these areas already at an early stage of the disease, most likely followed by hypometabolism and cortical atrophy during the course of disease progression (Buckner et al., 2005; Frisoni et al., 2010; Jack et al., 2010). Using graph analysis, Buckner et al. found the structures in the posterior midline, and in particular the PCC, to be an important "hub" in intrinsic cortical connectivity (Buckner et al., 2009). Their high neuronal activity might provoke increased amyloid-β production (Cirrito et al., 2005), possibly explaining the vulnerability of amyloid deposition in this region. Because the PCC and medial temporal cortex are both anatomically and functionally connected it is conceivable that amyloid deposition contributes to synaptic dysfunction and eventual neuronal loss in the hippocampus and surrounding cortical structures, and therefore contributes to memory impairment (Sperling et al., 2009).

Zhang et al. showed that the disruption of PCC connectivity intensified as the stage of AD progression increased (Zhang et al., 2010). In our study, regional FC values of MCI patients were numerically in between those of AD patients and controls (Fig. 3). Because MCI is considered as being a possible prodromal phase of AD, and MCI patients are known to have an increased risk of converting to AD compared with the healthy elderly population (Petersen et al., 2001), these findings were in line with our a priori expectations. After the exclusion of 1 outlier from the control group, a trend toward a significant difference in FC values was found between MCI patients and controls. Several studies found large proportions (i.e., approximately 30%) of clinically normal elderly to display increased amyloid deposition (Jack et al., 2009; Sperling et al., 2009), which appears to be associated with a decrease in DMN FC before any signs of cognitive impairment are detectable (Hedden et al., 2009; Mormino et al., 2011; Sheline et al., 2010). Although there was no additional information (e.g., molecular imaging) available for this specific control subject, incipient Alzheimer pathology might have caused increased variance of control FC values (Fig. 3), hampering differences between controls and MCI patients to reach statistical significance. Similarly, increased amyloid burden could have caused decreased FC in the sMCI group as well, possibly preventing sMCI and cMCI to reach statistical significance due to relatively low FC in some sMCI subjects.

Table 3
Associations of regional FC with cognitive function

Cognitive function	Across groups	Control	MCI	AD
MMSE	0.41***	0.14	−0.31	0.28
Digit span, forward [a]	0.17	0.09	0.18	−0.05
Digit span, backward [a]	0.28**	0.13	0.31	0.16
TMT A [a,b]	−0.37***	−0.09	−0.03	−0.37
Stroop, word [a,b]	−0.28*	0.04	−0.20	−0.27
Stroop, color [a,b]	−0.18	0.26	−0.04	−0.08
Stroop, color-word [b,c]	−0.28*	−0.16	−0.04	−0.18
RAVLT, immediate	0.27**	0.09	−0.21	0.06
RAVLT, delayed	0.25*	0.09	−0.29	−0.22
VAT [a]	0.32***	0.28	−0.08	−0.00
AT picture naming [c]	−0.01	−0.15	−0.05	−0.16
TMT B [b,c]	−0.34***	0.04	−0.23	−0.38
Category fluency [a]	0.26*	−0.14	−0.13	0.19
Rey figure copy [c]	0.35***	0.16	−0.19	0.61***

Data are presented as standardized β-values. Linear regression analyses (functional connectivity [FC], independent variable; neuropsychological test result, dependent variable) were carried out with correction for age and sex.

Key: AD, Alzheimer's disease; MCI, mild cognitive impairment; MMSE, Mini Mental State examination; RAVLT, Rey Auditory Verbal Learning Task; TMT, Trail Making TestVAT, Visual Association Test.

[a] Missing data of 1–3 subjects.

[b] Lower scores indicate better (faster) performance.

[c] Missing data of 4–8 subjects.

* $p < 0.05$.

** $p < 0.01$.

*** $p < 0.005$.

In this first study using rs-fMRI to compare DMN regional FC of sMCI and cMCI patients no differences were found between sMCI and cMCI patients. However, this could be explained by the small group sizes of the MCI subgroups. Furthermore, it is possible that the sMCI patients showing lowest regional FC values will still convert to AD after a longer clinical follow-up. Further studies in larger MCI samples are necessary to confirm these assumptions.

Although our main focus was on FC changes within the DMN, 2 other RSNs displayed FC changes in AD compared with controls as well. In the occipital regions of the secondary visual network a small region of lower FC was found. However, this result did not survive correction for gray matter atrophy. The network consisting of basal ganglia and cerebellum showed regional FC changes in AD in the deep gray matter of the brain, namely the right thalamus and putamen, and in the cerebellum. The cerebellum and the basal ganglia are anatomically interconnected (Bostan and Strick, 2010), supporting the idea that these subcortical structures form an integrated functional network. Besides being involved in motor function, the cerebellum and basal ganglia have an important role in cognitive function (Strick et al., 2009; Zhang et al., 2008). Furthermore, several studies have shown that especially the thalamus, but also the putamen, suffer volume loss during the disease progress of AD (Karas et al., 2004; Zarei et al., 2010), which is correlated with a decline in cognitive performance (Roh et al., 2011).

Finally, across diagnostic groups an association between lower regional FC and worse cognitive test performance was found for MMSE scores and several other neuropsychological tests. Within the AD group an association between FC and cognition was only found for the Rey Figure Copy test, most likely due to statistical power. However, because visuospatial capacities are tested with the Rey Figure Copy test, it is meaningful that these test results are strongly associated with posteromedial FC in AD, confirming the possible additional value of FC measures for clinical follow-up or as a measure for drug trial monitoring. Where amyloid deposition markers fail to display disease progression because amyloid markers reach a plateau very early in the disease process, functional MRI might prove to be a valuable measure.

A possible limitation of the current study is the influence of gray matter atrophy causing blood oxygen level-dependent (BOLD) signal alterations to be misinterpreted as FC alterations. Therefore a correction for gray matter atrophy was applied, using each subject's gray matter volume as a covariate in an additional dual regression analysis. Potentially more precise voxel-wise correction for gray matter atrophy (Oakes et al., 2007) could be hampered by misregistration of structural and functional images due to deformation of echo-planar images at 3T.

Further possible limitations of this study were the relatively small sample size of the MCI group, which might have caused a lack of statistical power to display decreases in regional FC in cMCI compared with sMCI when comparing both groups directly. Secondly, clinical follow-up time was too short to claim a definite separation between the sMCI and cMCI group. The MCI group used in our study was a heterogeneous group. No preselection of MCI patients was made based on assumable underlying AD pathology. Therefore, a significant part of the MCI group might not convert to AD (i.e., sMCI or frontotemporal lobar degeneration). However, with the current follow-up time it is not improbable that part of the sMCI group will still convert to AD (and thus actually belong to the cMCI group). Finally, the dual-regression technique uses the group ICA spatial maps for back-reconstruction purposes. This advantage, as described above, might at the same time be a limitation, because a commonality of spatial maps is assumed in order to obtain distinct subject-specific spatial maps. Therefore the results of our dual regression analysis will have to be compared with other techniques in future studies to assure that our results were not affected by the analysis technique, but solely caused by the disease itself.

In conclusion, these results show clinically meaningful changes in resting-state FC in AD patients. Although more studies in larger MCI groups are necessary to further explore early FC differences between sMCI and cMCI, rs-fMRI is a promising technique that can identify functional impairment in early Alzheimer's disease, and bridge the gap between molecular pathology (amyloid PET) and frank neurodegeneration with tissue loss (atrophy on MRI).

Disclosure statement

Mr. Schoonheim receives research support from the Dutch MS Research Foundation, grant number 08–650. Dr. Van Berckel receives research support from the American Health Assistance Foundation, Alzheimer Association, Internationale Stichting Alzheimer Onderzoek, the Center of Translational Molecular Medicine, and the Dutch Organisation for Scientific Research. Dr. Barkhof serves on the editorial boards of *Brain*, *European Radiology*, the *Journal of Neurology, Neurosurgery & Psychiatry*, the *Journal of Neurology*, *Multiple Sclerosis*, and *Neuroradiology* and serves as a consultant for Bayer-Shering Pharma, Sanofi-Aventis, Biogen-Idec, UCB, Merck-Serono, Jansen Alzheimer Immunotherapy, Baxter, Novartis, and Roche. There are no other actual or potential conflicts of interest to disclose.

The Ethical Review Board of the VU University Medical Center Amsterdam approved the study, and written informed consent was provided by all subjects or their lawful caregiver.

Acknowledgements

This study was sponsored by Alzheimer Center Amsterdam, Image Analysis Center and Neuroscience Campus, Amsterdam.

References

Bai, F., Watson, D.R., Yu, H., Shi, Y., Yuan, Y., Zhang, Z., 2009. Abnormal resting-state functional connectivity of posterior cingulate cortex in amnestic type mild cognitive impairment. Brain Res. 1302, 167–174.

Bai, F., Zhang, Z., Yu, H., Shi, Y., Yuan, Y., Zhu, W., Zhang, X., Qian, Y., 2008. Default-mode network activity distinguishes amnestic type mild cognitive impairment from healthy aging: a combined structural and resting-state functional MRI study. Neurosci. Lett. 438, 111–115.

Beckmann, C.F., DeLuca, M., Devlin, J.T., Smith, S.M., 2005. Investigations into resting-state connectivity using independent component analysis. Philos. Trans. R. Soc. Lond. B Biol. Sci. 360, 1001–1013.

Biswal, B., Yetkin, F.Z., Haughton, V.M., Hyde, J.S., 1995. Functional connectivity in the motor cortex of resting human brain using echo-planar MRI. Magn. Reson. Med. 34, 537–541.

Bostan, A.C., Strick, P.L., 2010. The cerebellum and basal ganglia are interconnected. Neuropsychol. Rev. 20, 261–270.

Buckner, R.L., Sepulcre, J., Talukdar, T., Krienen, F.M., Liu, H., Hedden, T., Andrews-Hanna, J.R., Sperling, R.A., Johnson, K.A., 2009. Cortical hubs revealed by intrinsic functional connectivity: mapping, assessment of stability, and relation to Alzheimer's disease. J. Neurosci. 29, 1860–1873.

Buckner, R.L., Snyder, A.Z., Shannon, B.J., LaRossa, G., Sachs, R., Fotenos, A.F., Sheline, Y.I., Klunk, W.E., Mathis, C.A., Morris, J.C., Mintun, M.A., 2005. Molecular, structural, and functional characterization of Alzheimer's disease: evidence for a relationship between default activity, amyloid, and memory. J. Neurosci. 25, 7709–7717.

Cirrito, J.R., Yamada, K.A., Finn, M.B., Sloviter, R.S., Bales, K.R., May, P.C., Schoepp, D.D., Paul, S.M., Mennerick, S., Holtzman, D.M., 2005. Synaptic activity regulates interstitial fluid amyloid-beta levels in vivo. Neuron 48, 913–922.

Cole, D.M., Beckmann, C.F., Long, C.J., Matthews, P.M., Durcan, M.J., Beaver, J.D., 2010. Nicotine replacement in abstinent smokers improves cognitive withdrawal symptoms with modulation of resting brain network dynamics. Neuroimage 52, 590–599.

Cordes, D., Haughton, V.M., Arfanakis, K., Carew, J.D., Turski, P.A., Moritz, C.H., Quigley, M.A., Meyerand, M.E., 2001. Frequencies contributing to functional connectivity in the cerebral cortex in "resting-state" data. AJNR Am. J. Neuroradiol. 22, 1326–1333.

Damoiseaux, J.S., Beckmann, C.F., Arigita, E.J., Barkhof, F., Scheltens, P., Stam, C.J., Smith, S.M., Rombouts, S.A., 2008. Reduced resting-state brain activity in the "default network" in normal aging. Cereb. Cortex 18, 1856–1864.

Damoiseaux, J.S., Rombouts, S.A., Barkhof, F., Scheltens, P., Stam, C.J., Smith, S.M., Beckmann, C.F., 2006. Consistent resting-state networks across healthy subjects. Proc. Natl. Acad. Sci. U. S. A. 103, 13848–13853.

Filippini, N., MacIntosh, B.J., Hough, M.G., Goodwin, G.M., Frisoni, G.B., Smith, S.M., Matthews, P.M., Beckmann, C.F., Mackay, C.E., 2009. Distinct patterns of brain activity in young carriers of the APOE-epsilon4 allele. Proc. Natl. Acad. Sci. U. S. A. 106, 7209–7214.

Folstein, M.F., Folstein, S.E., McHugh, P.R., 1975. "Mini-mental state". A practical method for grading the cognitive state of patients for the clinician. J. Psychiatr. Res. 12, 189–198.

Frisoni, G.B., Fox, N.C., Jack, C.R.J., Scheltens, P., Thompson, P.M., 2010. The clinical use of structural MRI in Alzheimer disease. Nat. Rev. Neurol. 6, 67–77.

Greicius, M.D., Krasnow, B., Reiss, A.L., Menon, V., 2003. Functional connectivity in the resting brain: a network analysis of the default mode hypothesis. Proc. Natl. Acad. Sci. U. S. A. 100, 253–258.

Greicius, M.D., Srivastava, G., Reiss, A.L., Menon, V., 2004. Default-mode network activity distinguishes Alzheimer's disease from healthy aging: evidence from functional MRI. Proc. Natl. Acad. Sci. U. S. A. 101, 4637–4642.

He, Y., Wang, L., Zang, Y., Tian, L., Zhang, X., Li, K., Jiang, T., 2007. Regional coherence changes in the early stages of Alzheimer's disease: a combined structural and resting-state functional MRI study. Neuroimage 35, 488–500.

Hedden, T., Van Dijk, K.R., Becker, J.A., Mehta, A., Sperling, R.A., Johnson, K.A., Buckner, R.L., 2009. Disruption of functional connectivity in clinically normal older adults harboring amyloid burden. J. Neurosci. 29, 12686–12694.

Jack, C.R., Jr., Knopman, D.S., Jagust, W.J., Shaw, L.M., Aisen, P.S., Weiner, M.W., Petersen, R.C., Trojanowski, J.Q., 2010. Hypothetical model of dynamic biomarkers of the Alzheimer's pathological cascade. Lancet Neurol. 9, 119–128.

Jack, C.R., Jr.., Lowe, V.J., Weigand, S.D., Wiste, H.J., Senjem, M.L., Knopman, D.S., Shiung, M.M., Gunter, J.L., Boeve, B.F., Kemp, B.J., Weiner, M., Petersen, R.C., Alzheimer's Disease Neuroimaging Initiative, 2009. Serial PIB and MRI in normal, mild cognitive impairment and Alzheimer's disease: implications for sequence of pathological events in Alzheimer's disease. Brain 132, 1355–1365.

Karas, G.B., Scheltens, P., Rombouts, S.A., Visser, P.J., van Schijndel, R.A., Fox, N.C., Barkhof, F., 2004. Global and local gray matter loss in mild cognitive impairment and Alzheimer's disease. Neuroimage 23, 708–716.

Lindeboom, J., Schmand, B., Tulner, L., Walstra, G., Jonker, C., 2002. Visual association test to detect early dementia of the Alzheimer type. J. Neurol. Neurosurg., Psychiatry 73, 126–133.

McKhann, G., Drachman, D., Folstein, M., Katzman, R., Price, D., Stadlan, E.M., 1984. Clinical diagnosis of Alzheimer's disease: report of the NINCDS-ADRDA Work Group under the auspices of Department of Health and Human Services Task Force on Alzheimer's Disease. Neurology 34, 939–944.

Mormino, E.C., Smiljic, A., Hayenga, A.O., Onami, H., Greicius, M.D., Rabinovici, G.D., Janabi, M., Baker, S.L., Yen, V., Madison, C.M., Miller, B.L., Jagust, W.J., 2011. Relationships between beta-amyloid and functional connectivity in different components of the default mode network in aging. Cereb. Cortex, doi: 10.1093/cercor/bhr025.

Morris, J.C., 1993. The Clinical Dementia Rating (CDR): current version and scoring rules. Neurology 43, 2412–2414.

Neary, D., Snowden, J.S., Gustafson, L., Passant, U., Stuss, D., Black, S., Freedman, M., Kertesz, A., Robert, P.H., Albert, M., Boone, K., Miller, B.L., Cummings, J., Benson, D.F., 1998. Frontotemporal lobar degeneration: a consensus on clinical diagnostic criteria. Neurology 51, 1546–1554.

Nichols, T.E., Holmes, A.P., 2002. Nonparametric permutation tests for functional neuroimaging: a primer with examples. Hum. Brain Mapp. 15, 1–25.

Oakes, T.R., Fox, A.S., Johnstone, T., Chung, M.K., Kalin, N., Davidson, R.J., 2007. Integrating VBM into the General Linear Model with voxelwise anatomical covariates. Neuroimage 34, 500–508.

Osterrieth, P.A., 1944. The test of copying a complex figure: A contribution to the study of perception and memory. Arch. Psychol. 30, 286–356.

Petersen, R.C., Stevens, J.C., Ganguli, M., Tangalos, E.G., Cummings, J.L., DeKosky, S.T., 2001. Practice parameter: early detection of dementia: mild cognitive impairment (an evidence-based review). Report of the Quality Standards Subcommittee of the American Academy of Neurology. Neurology 56, 1133–1142.

Qi, Z., Wu, X., Wang, Z., Zhang, N., Dong, H., Yao, L., Li, K., 2010. Impairment and compensation coexist in amnestic MCI default mode network. Neuroimage 50, 48–55.

Raichle, M.E., MacLeod, A.M., Snyder, A.Z., Powers, W.J., Gusnard, D.A., Shulman, G.L., 2001. A default mode of brain function. Proc. Natl. Acad. Sci. U. S. A. 98, 676–682.

Rey, A., 1964. L'examen Clinique en Psychologie, second ed. Presses Universitaires de France. Paris.

Roh, J.H., Qiu, A., Seo, S.W., Soon, H.W., Kim, J.H., Kim, G.H., Kim, M.J., Lee, J.M., Na, D.L., 2011. Volume reduction in subcortical regions according to severity of Alzheimer's disease. J. Neurol. 258, 1013–1020.

Roosendaal, S.D., Schoonheim, M.M., Hulst, H.E., Sanz-Arigita, E.J., Smith, S.M., Geurts, J.J., Barkhof, F., 2010. Resting state networks change in clinically isolated syndrome. Brain 133, 1612–1621.

Schölvinck, M.L., Maier, A., Ye, F.Q., Duyn, J.H., Leopold, D.A., 2010. Neural basis of global resting-state fMRI activity. Proc. Natl. Acad. Sci. U. S. A. 107, 10238–10243.

Sheline, Y.I., Raichle, M.E., Snyder, A.Z., Morris, J.C., Head, D., Wang, S., Mintun, M.A., 2010. Amyloid plaques disrupt resting state default mode network connectivity in cognitively normal elderly. Biol. Psychiatry 67, 584–587.

Sluimer, J.D., van der Flier, W.M., Karas, G.B., van Schijndel, R., Barnes, J., Boyes, R.G., Cover, K.S., Olabarriaga, S.D., Fox, N.C., Scheltens, P., Vrenken, H., Barkhof, F., 2009. Accelerating regional atrophy rates in the progression from normal aging to Alzheimer's disease. Eur. Radiol. 19, 2826–2833.

Smith, S.M., Nichols, T.E., 2009. Threshold-free cluster enhancement: addressing problems of smoothing, threshold dependence and localisation in cluster inference. Neuroimage 44, 83–98.

Smith, S.M., Zhang, Y., Jenkinson, M., Chen, J., Matthews, P.M., Federico, A., De Stefano, N., 2002. Accurate, robust, and automated longitudinal and cross-sectional brain change analysis. Neuroimage 17, 479–489.

Sorg, C., Riedl, V., Mühlau, M., Calhoun, V.D., Eichele, T., Läer, L., Drzezga, A., Förstl, H., Kurz, A., Zimmer, C., Wohlschläger, A.M., 2007. Selective changes of resting-state networks in individuals at risk for Alzheimer's disease. Proc. Natl. Acad. Sci. U. S. A. 104, 18760–18765.

Sperling, R.A., LaViolette, P.S., O'Keefe, K., O'Brien, J., Rentz, D.M., Pihlajamaki, M., Marshall, G., Hyman, B.T., Selkoe, D.J., Hedden, T., Buckner, R.L., Becker, J.A., Johnson, K.A., 2009. Amyloid deposition is associated with impaired default network function in older persons without dementia. Neuron 63, 178–188.

Strick, P.L., Dum, R.P., Fiez, J.A., 2009. Cerebellum and nonmotor function. Annu. Rev. Neurosci. 32, 413–434.

Stroop, J.R., 1935. Studies of interference in serial verbal reactions. J. Exp. Psychol. 18, 643–662.

Tolboom, N., van der Flier, W.M., Yaqub, M., Koene, T., Boellaard, R., Windhorst, A.D., Scheltens, P., Lammertsma, A.A., van Berckel, B.N., 2009. Differential association of [11C]PIB and [18F]FDDNP binding with cognitive impairment. Neurology 73, 2079–2085.

Verhage, F., 1964. Intelligence and Age: Study With Dutch People Aged 12 to 77 [in Dutch]. van Gorcum, Assen.

Wang, K., Liang, M., Wang, L., Tian, L., Zhang, X., Li, K., Jiang, T., 2007. Altered functional connectivity in early Alzheimer's disease: a resting-state fMRI study. Hum. Brain Mapp. 28, 967–978.

Wang, L., Zang, Y., He, Y., Liang, M., Zhang, X., Tian, L., Wu, T., Jiang, T., Li, K., 2006. Changes in hippocampal connectivity in the early stages of Alzheimer's disease: evidence from resting state fMRI. Neuroimage 31, 496–504.

Wechsler, D., 1997. Wechsler Adult Intelligence Scale, third ed. San Antonio, TX: The Psychological Corp.

Zarei, M., Patenaude, B., Damoiseaux, J., Morgese, C., Smith, S., Matthews, P.M., Barkhof, F., Rombouts, S.A., Sanz-Arigita, E., Jenkinson, M., 2010. Combining shape and connectivity analysis: an MRI study of thalamic degeneration in Alzheimer's disease. Neuroimage 49, 1–8.

Zhang, D., Snyder, A.Z., Fox, M.D., Sansbury, M.W., Shimony, J.S., Raichle, M.E., 2008. Intrinsic functional relations between human cerebral cortex and thalamus. J. Neurophysiol. 100, 1740–1748.

Zhang, H.Y., Wang, S.J., Liu, B., Ma, Z.L., Yang, M., Zhang, Z.J., Teng, G.J., 2010. Resting brain connectivity: changes during the progress of Alzheimer disease. Radiology 256, 598–606.

Zhang, H.Y., Wang, S.J., Xing, J., Liu, B., Ma, Z.L., Yang, M., Zhang, Z.J., Teng, G.J., 2009. Detection of PCC functional connectivity characteristics in resting-state fMRI in mild Alzheimer's disease. Behav. Brain Res. 197, 103–108.

Zhou, J., Greicius, M.D., Gennatas, E.D., Growdon, M.E., Jang, J.Y., Rabinovici, G.D., Kramer, J.H., Weiner, M., Miller, B.L., Seeley, W.W., 2010. Divergent network connectivity changes in behavioural variant frontotemporal dementia and Alzheimer's disease. Brain 133, 1352–1367.